Engenharia Agrícola

ISSN: 1809-4430 (on-line)

www.engenhariaagricola.org.br

Scientific Paper

Doi: http://dx.doi.org/10.1590/1809-4430-Eng.Agric.v42n5e20220075/2022

RESEARCH ON WIND PRESSURE DISTRIBUTION OF PLASTIC GREENHOUSES IN VALLEY TOPOGRAPHY

Jing Xu[1*], Guifeng He[1], Xiaoying Ren[1], Zhikang Hu[1]

[1*]Corresponding author. College of Water Resources and Civil Engineering, China Agricultural University, Beijing 100083, China. E-mail: xujing@cau.edu.cn | ORCID ID: https://orcid.org/0000-0002-2875-3675

KEYWORDS

Plastic greenhouse, valley area, wind pressure distribution coefficient, numerical simulation, fitting formula.

ABSTRACT

As the wind pressure distribution on plastic greenhouses in valley areas is different from that of greenhouses on plains, it is necessary to find out the variation trend of the wind pressure coefficient on greenhouses in the valley areas. Based on the 'Realizable k-ε turbulence' model, the wind pressure characteristics on plastic greenhouses located in valley and plain areas are studied by using the verified numerical simulation method. The wind pressures on greenhouses and the corresponding fitting formula are obtained for different distances between the greenhouse and the foot of the mountain with a 0-degree wind angle. The results show that, with an increase of distance to the mountain, the positive wind pressure on the windward side of a plastic greenhouse increases and the negative wind pressure on the leeward side, roof surface and crosswind sides of the greenhouse decreases. The results from the proposed formulae are very close to those derived from the numerical simulation method, and the relative errors are all within 10%. The influence of canyon wind on the wind pressure distribution on plastic greenhouses should be considered in the design. This research can provide a reference for the wind resistance design of plastic greenhouses built in valley areas.

INTRODUCTION

With the introduction of the greenhouse modernization policy proposed by the Tibet Autonomous Region Government, Tibet is vigorously promoting the construction of plastic greenhouses. A plastic greenhouse is a simple structure, which is sensitive to strong wind and heavy snow load, and damage or collapse occurs from time to time. For mountainous and high-altitude regions, wind characteristics in the valley are different from those in plain areas. The wind characteristics can reflect the distribution of wind pressure on greenhouses. The load code for the design of building structures in China (GB 50009-2012) prescribes the adjustment of the wind pressure coefficient of buildings located on hillsides and mountain peaks, but there are no relevant provisions for the valley effect on the wind pressure coefficient of buildings. Therefore, it is important to study the effect of wind pressure coefficient on plastic greenhouses in the valleys in Tibet.

Due to the complex action of wind on greenhouses, the aerodynamic interference between them is difficult to predict, which leads to difficulty in obtaining the wind pressure coefficient from theoretical calculations. The field experimental test method, wind tunnel test method and numerical simulation method are adopted to determine the wind pressure coefficient. Among them, field measurement (Richards & Hoxey, 2012; Charisi et al., 2019) is the most direct and accurate method, using a full-scale model. However, the on-site measurement method is easily affected by weather and equipment and the obtained results are only applicable to the prevailing conditions.

Wind tunnel tests have been widely used as an accurate alternative method to conduct aerodynamic studies and to obtain sufficient quantitative data (Lee et al., 2003). Wind tunnel tests (Paepe et al., 2013; Moriyama et al., 2015; Bautista et al., 2016; Kwon et al., 2016) are conducted to study the effects of wind angle and ridge height on the distribution of the wind pressure coefficient on greenhouses,

[1] College of Water Resources and Civil Engineering, China Agricultural University, Beijing 100083, China.

Area Editor: Héliton Pandorfi
Received in: 5-12-2022
Accepted in: 9-5-2022

by using different scale models. Wind tunnel tests also have experimental limitations: 1) a limited number of channels for simultaneous measurement, 2) limited greenhouse model size due to the blockage ratio, 3) cost of manufacturing of a greenhouse model under various experimental conditions, and 4) high time and labor-consumption costs (Kim et al. 2017a).

With the rapid development of computational fluid dynamics (CFD), numerical methods have been effectively applied and broadly used to obtain reliable quantitative and qualitative data. Kim et al. (2017b) estimated the pressure coefficients of multi-span greenhouses, which are typical in South Korea, using the developed CFD model. Vieira Neto & Soriano (2020) used computational fluid dynamics (CFD) models to obtain the pressure coefficients in greenhouses with height/span ratios of 0.3 and 0.6.

Meanwhile, the spatial distribution of the wind field, wind speed distribution and other wind field characteristics in valley areas, were also studied. Blocken et al. (2015) used CFD to simulate the complex wind field at a narrow entrance surrounded by irregular hills. Yao et al. (2016) and Shen et al. (2016) adopted CFD numerical simulation to study the characteristics of wind fields and the acceleration effect of typical locations in canyons. Abdullah et al. (2018) studied the pressure distribution and streamlines around an isolated house, by considering the effect of terrain characteristics, as well as the topographic features, such as flats, depressions, ridges and valleys.

Above all, most studies have been carried out on greenhouses situated on the plain areas or the wind characteristics of mountain fields alone. The wind pressure distribution coefficient for plastic greenhouses in valley areas needs to be studied. In this paper, a numerical simulation method is used to estimate the wind pressure on plastic greenhouses in valley areas, based on the verified Realizable k-ε turbulence model. The effect of the valley distance between two mountains on the pressure is also studied and compared with the wind pressure distribution on the greenhouse in the plain area; this plays an important role in understanding the effect of wind pressure characteristics and its distribution on plastic greenhouses in the valley areas.

MATERIAL AND METHODS

Wind pressure coefficient

According to Bernoulli's principle, the wind pressure coefficient can be defined as the ratio of the net wind pressure at any measuring point on the surface of a building to the average dynamic pressure of the upstream wind far in the front of the building, the expression is (GB 50009-2012, 2012):

$$C_P = \frac{p_p - p_\infty}{\frac{1}{2}\rho V_\infty^2} \quad (1)$$

In Equation (1),

C_p is the average wind pressure coefficient at point p;

p_p is the static pressure at point p, kN/m^2;

p_∞ is the static pressure at the far forward upstream reference height, kN/m^2;

ρ is air mass density (according to the field test in Lhasa, Tibet, ρ is equal to 0.7548 kg/m^3), and

V_∞ is the average wind speed at the reference height, which is generally the average wind speed at a height of 10 m, m/s.

Weighted value of wind pressure distribution coefficient

According to the Chinese code, the average wind pressure coefficient on the surface is generally used as the wind pressure distribution coefficient. The wind pressure distribution coefficient can be obtained by taking the weighted average of the product of the wind pressure coefficient of the measuring point on the surface and the surface area of the measuring point. The expression is (GB 50009—2012, 2012):

$$\mu_s = \frac{\sum_i C_p A_i}{A} \quad (2)$$

In Equation (2),

μ_s is the shape coefficient;

A_i is the surface area of the measuring area, m^2, and

A is the total area of the surface, m^2.

MODEL ESTABLISHMENT AND VERIFICATION

Model parameters

Structural parameters

Most of the Tibetan mountains feature precipitous summits and steep slopes. Considering the complexity of establishing a real valley terrain model, the mountain model is simplified as a cosine mountain model $z = H[1 + cos(\pi r/2L_1)/2]$ (Chen, 2007), which has a larger slope than other mountain models, to study the wind load characteristics on a greenhouse in a typical valley. In this model, $r = \sqrt{x^2 + y^2}$, H is the height of the mountain (H = 100 m), and L_1 is the horizontal distance from the top of the mountain to the middle of the mountain (L_1 = 100 m). The diameter D of the mountain model is 400 m, the length of the ridge is 300 m, and the slope is 0.5, as shown in Figure 1 (a). The greenhouse was placed between two mountains and the horizontal distance from the bottom of the mountain to the greenhouse is d, as shown in Figure 1 (a). The arched plastic greenhouse structure was selected from the more widely used dimensional models in China, whose size is: length of 44 m, span of 7 m, height of 3.5 m, and canopy shoulder height of 1.6 m. The rise-span ratio is 0.27, as shown in Figure 1 (b).

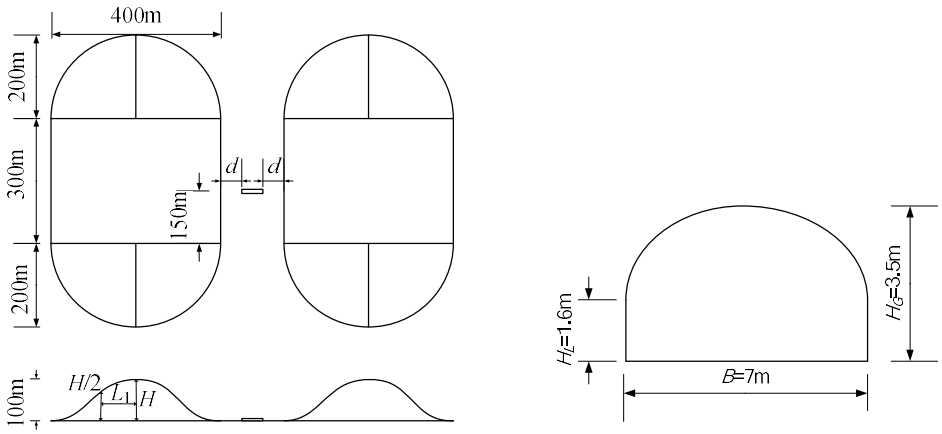

(a) Diagrammatic figure of a mountain (b) Dimensions of the greenhouse

FIGURE 1. Dimensions of the mountain and greenhouse.

Fluid domain and grid meshing

According to the dimensions of the plastic greenhouse and the mountain, the flow field size and model placement location are shown in Figure 2. 6*H* is taken for the upstream and both sides of the flow field, 7*H* is taken for the height direction, and 15*H* is taken for the downstream of the flow field (Kim et al., 2017a), in which *H* is the height of the mountain and equal to 100 m. The model was placed at the front third of the wind field calculation domain and the blocking rate is less than 3%, to reduce the interaction between the fluid and the boundary (Sun, 2011).

In order to improve the calculation efficiency and accuracy of the model, it is imported into the Fluent Meshing module for grid division, in which the grids around the greenhouse and mountain are locally densified and the boundary layer is set. To verify the grid independence in the simulation, five grid independence tests were conducted, in which the size of the surface grid of the greenhouse is *l*/10, *l*/15, *l*/20, *l*/25, and *l*/30, respectively, as shown in Table 1. Overall, the grid size of the greenhouse and the mountain takes *l*/20 of the shortest side length of the model, of which the minimum size of the grid of the greenhouse surface is 0.1 m, and the minimum size of the mountain surface is 5 m. In order to make the wind pressure on the surface of the greenhouse more accurate, the boundary layer is set to 6 layers, and the minimum size of the first layer grid is set to 1.0×10^{-2} m. As an emerging mesh technology, polyhedron mesh has many advantages (Feng et al., 2016). So, in the model, the polyhedron meshes are selected and the number of grids is about 1.5 million, as shown in Figure 3.

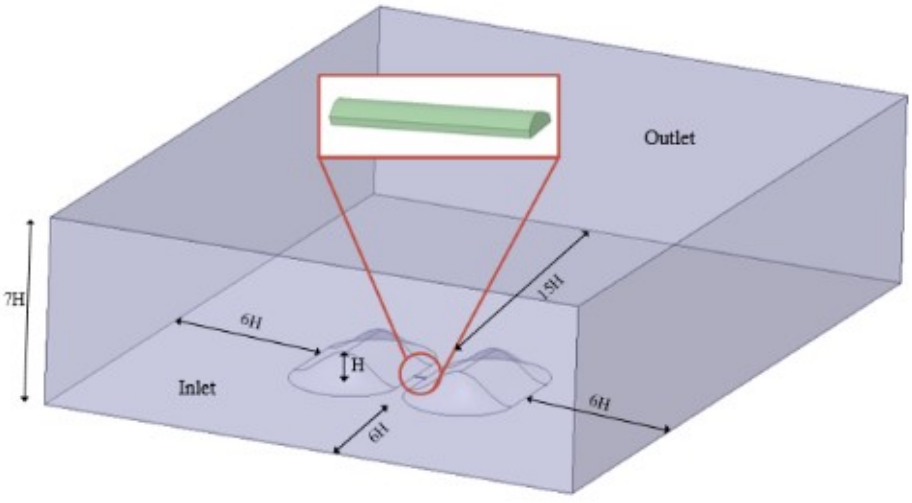

FIGURE 2. Fluid domain and model diagram.

TABLE 1. Grid size properties.

Mesh size classification	*l*/10	*l*/15	*l*/20	*l*/25	*l*/30
Meshing size of greenhouse (m)	0.160	0.106	0.080	0.064	0.053
Meshing size of mountain (m)	10.000	6.667	5.000	4.000	3.333
Total number of grids	639114	1258233	1917194	2860792	4028784

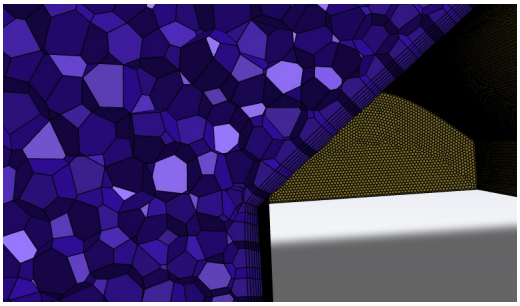

(a) Mesh in wall boundary layer

(b) Volume mesh in fluid domain

FIGURE 3. Polyhedron mesh diagram.

Boundary conditions in wind field

The inflow boundary condition is defined as a velocity inlet, where velocity V has an exponential distribution. The calculated profiles were applied as boundary conditions in the CFD simulation via user-defined functions (UDF). The expression of the exponential wind speed profile is (GB 5009-2012, 2012):

$$V = V_0\left(\frac{Z}{Z_0}\right)^{\alpha} \tag{3}$$

In Equation (3),

Z is the height corresponding to wind speed V;

Z_0 is the reference height，Z_0=10 m；

V_0 is the average wind speed at Z_0, V_0=13.3 m/s, and

α is the roughness coefficient. In accordance with the load code for the design of building structures in China (GB 5009-2012, 2012), Tibet conforms to a class B landform, therefore α=0.16 (GB 5009-2012, 2012).

Since there is no clear definition of turbulence intensity in the current Chinese code, the expressions of turbulence kinetic energy k and turbulence dissipation rate ε are obtained based on the Japanese code (AIJ-RLBC, 2015):

$$k = 1.5\left[VI\left(Z\right)\right]^2 \tag{4}$$

$$\varepsilon = \frac{0.09^{0.75}k^{1.5}}{l} \tag{5}$$

in which:

$I(Z)$ is turbulence intensity, and l is the characteristic scale of turbulence at the inlet, whose equations are:

$$I\left(Z\right) = \begin{cases} 0.23 & Z \le 5\text{ m} \\ 0.1\left(\dfrac{Z}{350}\right)^{\alpha} & 5\text{ m} < Z \le 350\text{ m} \end{cases} \tag{6}$$

$$l = 100 \times \left(\frac{Z}{350}\right)^{0.5} \tag{7}$$

The outlet condition is termed ‘Pressure-outlet’ and is where the normal gradient of any physical quantity of the flow field along the outlet direction is zero. Symmetrical boundaries are adopted at the top and both sides of the fluid domain, while non-sliding walls are adopted for the mountains and greenhouse at the bottom of the fluid domain. The Realizable k-ε turbulence model, which has been widely used to simulate the wind pressure in valley areas (Xiao et al., 2009; Zhu et al., 2011; Yao, 2014), is adopted. A scalable wall function can produce consistent results for grids of arbitrary refinement and is always used in the simulation. In the iterative calculation, judge whether the flow field enters the steady state based on the change of the pressure field of the shed body.

Model validation

To verify the reliability of the Realizable k-ε turbulence model and the proposed meshing method, the greenhouse model tested by Kwon et al. (2016) is simulated, and the surface wind pressure coefficients of plastic greenhouses at 0° and 90° wind angle are obtained. The simulation results are compared with those from the wind tunnel tests (Kwon et al., 2016). The comparison results are shown in Figure 4 and Figure 5.

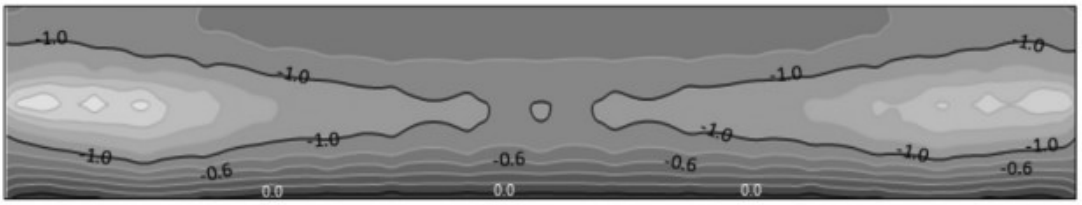

(a) Test results from Kwon et al. (2016)

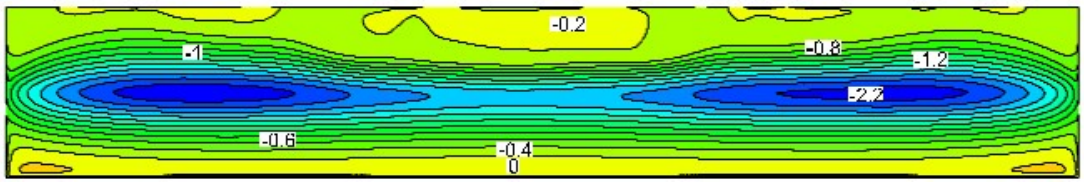

(b) Simulation results

FIGURE 4. Comparison results at 0° wind angle.

(a) Test results from Kwon et al. (2016)

(b) Simulation results

FIGURE 5. Comparison results at 90° wind angle.

According to the comparisons in Figure 4 and Figure 5, the results obtained from the simulation method are basically consistent with those from wind tunnel testing (Kwon et al., 2016) and the maximum positive pressure and maximum negative pressure positions and values are the same for the two methods. The wind pressure coefficient obtained in this paper is more detailed than the value obtained from wind tunnel testing. In summary, the Realizable k-ε turbulence model and meshing method proposed in this paper are feasible.

Model partition

Firstly, the Realizable k-ε turbulence model is used to simulate the wind pressure distribution of a single greenhouse in a plain area; the distribution is shown in Figure 6. In combination with the wind pressure distribution on the surface of the greenhouse and the structural characteristics of the greenhouse in Figure 6, the greenhouse is divided into different zones. When the wind direction angle is 0°, the surface of the greenhouse is divided into several parts, and the detailed zoning is shown in Figure 7. In Figure 7, F, T, B and W represent windward surface, roof surface, leeward surface and lateral surface; L, M, and R represent left, middle and right.

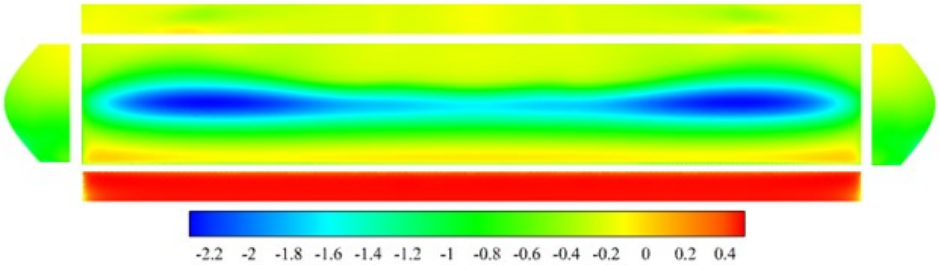

FIGURE 6. Numerical simulation results of single shed in plain area with a wind direction of 0°.

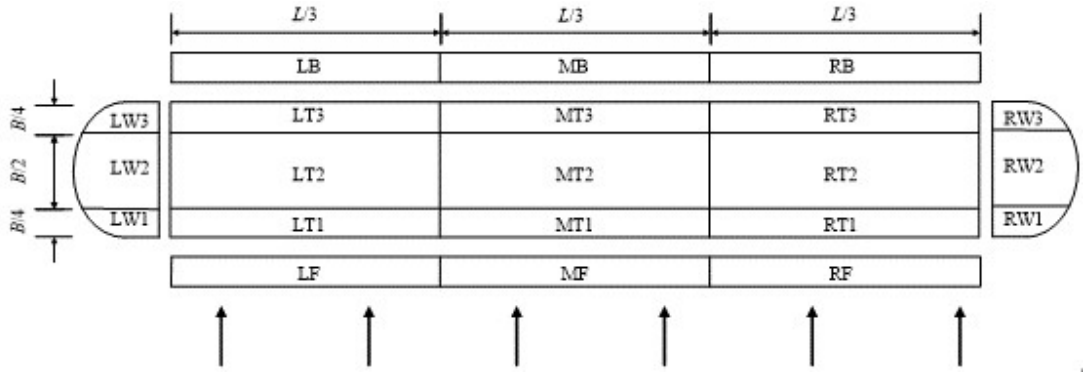

FIGURE 7. Zoning chart of greenhouse with a wind direction of 0°.

RESULTS AND DISCUSSION

Influence on wind pressure distribution coefficient of a greenhouse

The streamline diagram and wind speed distribution diagram are shown in Figure 8. Figure 9 shows the wind pressure distribution for a greenhouse when the greenhouse is located in a valley and on a plain area. In the valley area, the horizontal distance *d* between the greenhouse and the bottom of the mountain is equal to 0, 50, 150, 250, 350, 500, 700, and 900 m, respectively. According to the zoning diagram in Figure 7, the weighted wind pressure coefficients are derived based on [eq. (2)] and Figure 9. The relations between the wind pressure coefficient of the greenhouse located in the valley area and the horizontal distance *d*, are shown in Figure 10~13. The curves between the ratio of wind pressure coefficient in the valley area to that in the plain area and the ratio of the distance *d* to mountain height *H* are shown in Figure 14. The wind pressure coefficients of the greenhouse located on the plain are given in Table 2.

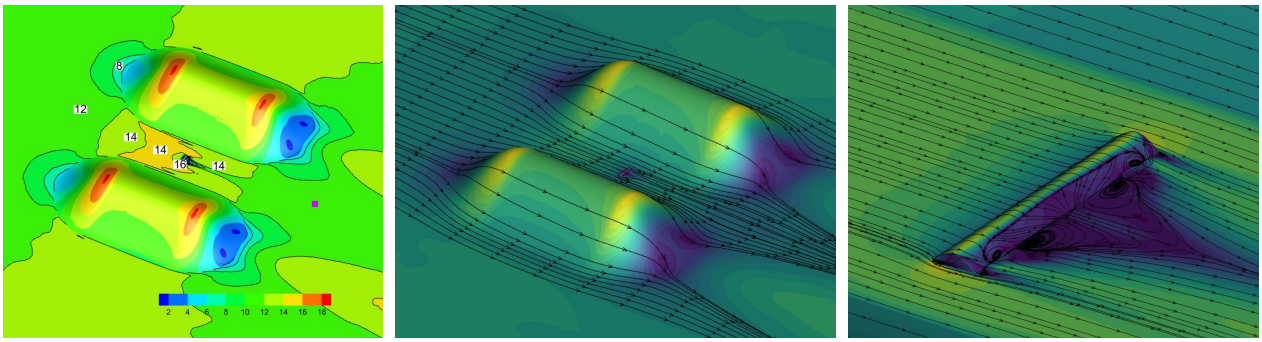

(a) (b) (c)

(a) Wind speed distribution in the valley (unit: m/s); (b) Flow field distribution with *d*=50 m; (c) Details of flow field on the surface of the greenhouse where *d*=50 m

FIGURE 8. Flow field distribution.

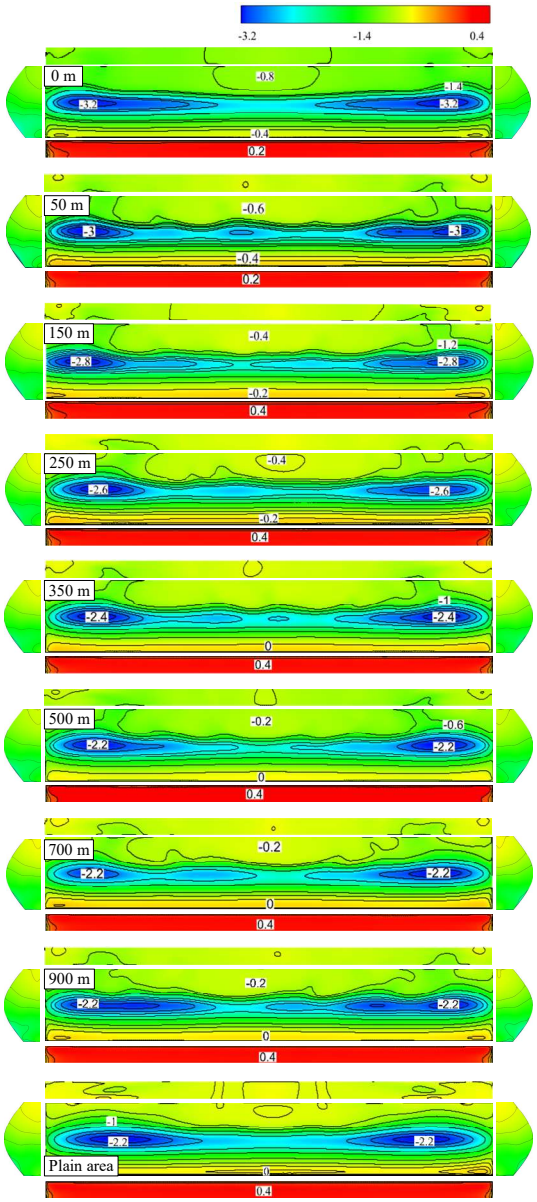

d = 0, 50, 150, 250, 350, 500, 700, and 900 m and in plain terrain.

FIGURE 9. Wind pressure distribution on the greenhouse in valley terrain when.

TABLE 2. Wind pressure distribution coefficient of greenhouse in plain terrain.

Location	MF	LF(RF)	LW1(RW1)	LW2(RW2)	LW3(RW3)	LB(RB)	MB
Plain terrain	0.568	0.555	-0.856	-0.523	-0.176	-0.213	-0.187
	LT1(RT1)	LT2(RT2)	LT3(RT3)	MT1	MT2	MT3	
	-0.279	-1.420	-0.352	-0.260	-1.100	-0.213	

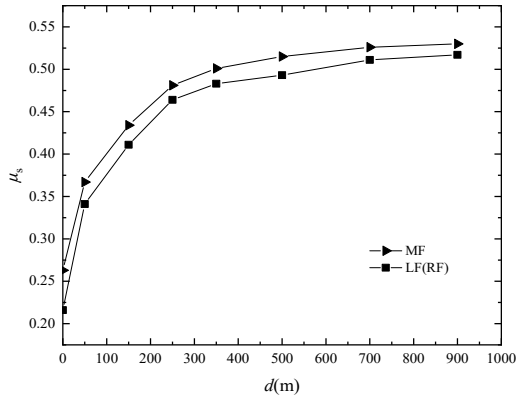

FIGURE 10. Wind pressure distribution coefficient on windward surface of greenhouse.

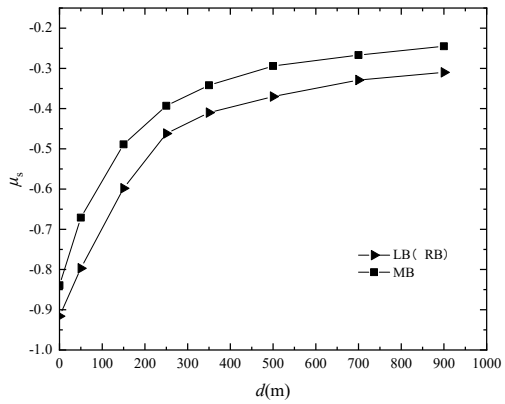

FIGURE 11. Wind pressure distribution coefficient on leeward surface of greenhouse.

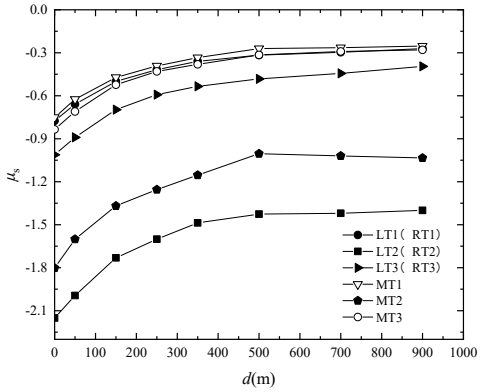

FIGURE 12. Wind pressure distribution coefficient on roof surface of greenhouse.

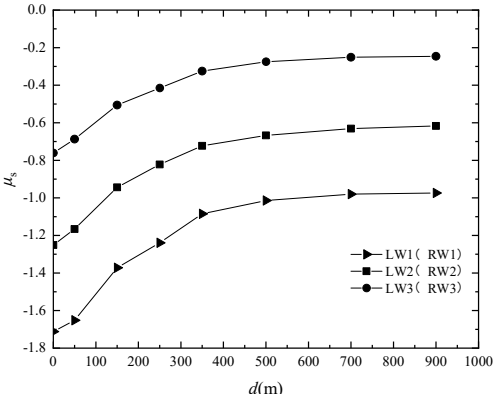

FIGURE 13. Wind pressure distribution coefficient on lateral surface of greenhouse.

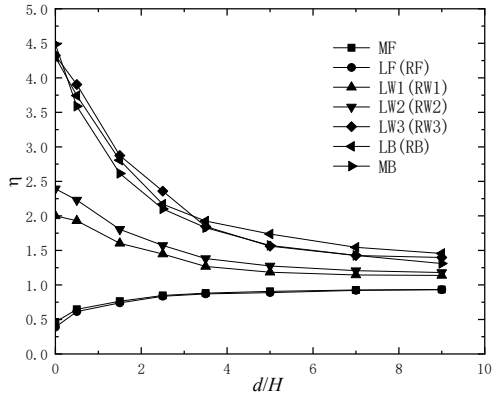

(a) Windward surface, leeward surface and lateral surface

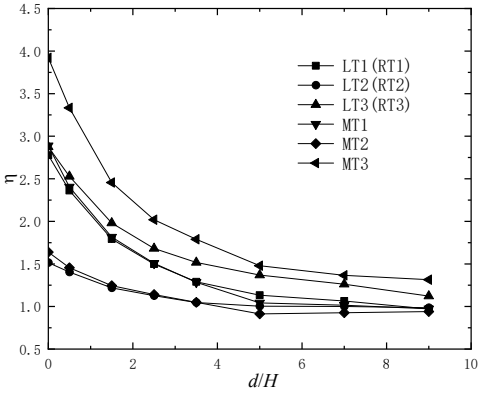

(b) Roof surface

FIGURE 14. Ratio of wind pressure coefficients of the greenhouse.

Analysis of numerical simulation results

As shown in Figure 8(a), when the wind passes through the mountains, the canyon wind is formed and results in an increase in wind speed, which is different from that when there is no shelter on the plain area. As can be seen from Figure 9, for a greenhouse located in a valley area, that the maximum positive wind pressure occurs on the windward side of the greenhouse; the maximum negative pressure occurs at both ends of the roof surface and large suction occurs on both the lateral and leeward surfaces. The reason for this is that, when the wind is blocked by the greenhouse, the wind will separate on the windward side of the roof surface and result in the formation of a columnar vortex; the wind diverts through the lateral surface of the greenhouse, which results in a large flow velocity and suction on the lateral surface. When the wind passes through the leeward area of the greenhouse, a swirling wake forms, resulting in a vortex on the surface of the greenhouse, as shown in Figure 8(c). The positive pressure on the windward side of the greenhouse increases with the increase in distance between the foot of the mountain and the greenhouse, while the maximum negative pressure on the leeward side, roof surface and crosswind surface decreases with the increase in distance. When the distance between the mountain and the greenhouse is within 500 m, the wind

pressure on any of the greenhouse surfaces changes. When the distance is greater than 500 m, the change of wind pressure tends to be flat, and when the distance reaches a certain value, the wind pressure values on all sides of the greenhouse tend to be close to the wind pressure value of a greenhouse in a plain area, as shown in Figure 9, Figure 14, and Table 2.

Figure 10 shows that the windward side of the greenhouse has positive pressure. The values of wind pressure in the region MF, LF and RF are not very different, and the value in region MF is slightly larger. When the foot of the mountain is 0 m away from the greenhouse, the wind pressure coefficients in the MF and LF/RF areas are 0.263 and 0.216, respectively. This is 0.46 and 0.39 times those of the greenhouse in the plain area, indicating that the wind pressure coefficients on the windward side in valley areas are smaller than those in the plain area.

As shown in Figure 11, the wind load on the leeward side of the greenhouse causes suction. The wind pressures in the LB, RB and MB areas are almost the same and the wind pressure in the MB area is slightly smaller. When the foot of the mountain is 0 m away from the greenhouse, the wind pressure coefficients in region MB and LB/RB are -0.839 and -0.916 respectively, which are 4.49 and 4.30 times higher than those in the plain area, indicating that the influence of valley wind on the wind pressure on the leeward side of the greenhouse is greater than that in the plain area.

As Figure 12 shows, the wind load on the roof side of the greenhouse causes suction. The wind pressure value in LT2/RT2 is the largest, followed by the values in MT2, then LT3/RT3 and, finally, the values in MT1, MT3 and LT1/RT1 are roughly the same and the smallest. When the foot of the mountain is 0 m away from the greenhouse, the wind pressure coefficients in areas LT2/RT2, MT2, LT3/RT3, MT1, LT1/RT1 and MT3 are -2.151, -1.802, -1.012, -0.751, -0.775 and -0.835 respectively, which are 1.51, 1.64, 2.88, 2.89, 2.78 and 3.92 times higher than those of the greenhouse on the plains. This indicates that the wind pressure coefficient near the leeward side of the roof surface is most affected by the valley wind.

Figure 13 shows that both lateral surfaces of the greenhouse are subject to negative pressure loading. The negative pressure in area LW1/RW1 is the largest, the pressure in area LW2/RW2 is the second largest, and the pressure in area LW3/RW3 is the smallest. When the distance between the foot of the mountain and the greenhouse is 0 m, the wind pressure coefficients in areas LW1/RW1, LW2/RW2 and LW3/RW3 are -1.712, -1.251 and -0.761 respectively, which are 2.0, 2.39 and 4.32 times that of the greenhouse in the plains region. The lateral wind pressure near the leeward side of the greenhouse is most affected by valley wind.

Fitting formula

The fitting formula between the wind pressure distribution coefficient μ_s of the plastic greenhouse and the horizontal distance d is proposed based on Figure 10~13, which can be expressed as:

$$\mu_s = A - BC^d \quad (8)$$

A, B and C are the respective values of the curve fitting coefficients.

The fitting coefficients A, B, and C for the windward surface, leeward surface, roof surface and lateral surface of the plastic greenhouse are given in Table 3. The relative errors between the results from each fitting formula and the results shown in Figure 10~13 are all within 10%, indicating the correctness of the fitting formulas.

TABLE 3. Values of fitting coefficients.

Coefficient	LW1/MT2	LW2	LW3	MF/LF/RF	LB/RB	MB/MT1	LT1/RT1/MT3	LT2/RT2	LT3/RT3
A	-0.965	-0.597	-0.226	0.516	-0.311	-0.252	-0.277	-1.389	-0.407
B	0.808	0.674	0.551	0.266	0.613	0.537	0.528	0.773	0.603
C	0.995								

CONCLUSIONS

In this paper, the verified CFD simulation method is used to simulate the wind pressure distribution coefficient of plastic greenhouses located in valley areas with 0° of wind direction. The conclusions are as follows:

(1) The positive wind pressure coefficient of the windward side of the plastic greenhouse increases with the increase of the distance between two mountains, while the negative wind pressure coefficient of the leeward side, roof surface and two lateral surfaces decreases. The wind pressure coefficient of each region changes significantly within 500 m of mountain spacing, and the change tends to be gradually stable when the mountain spacing is greater than 500 m.

(2) When the horizontal distance between the foot of the mountain and the plastic greenhouse is 0 m, the wind pressure coefficient of the windward side in the valley area is smaller than that in the plain area, indicating that the wind in the valley is beneficial to the stress on the windward side of the plastic greenhouse. The pressure of the valley wind on the leeward side, the crosswind side near the leeward side and the roof near the leeward side is different from that in the plain area, indicating that the valley wind has a great influence on the wind pressure of the areas near the leeward side. The wind pressure coefficient in other regions is also larger than that in the plain areas. Therefore, the effect of valley wind cannot be ignored.

(3) The fitting formula can better calculate the wind pressure distribution coefficient of a greenhouse and can provide a theoretical calculation basis for the corresponding specifications.

ACKNOWLEDGMENTS

This study was supported by the National Natural Science Foundation of China (Grant No. U20A2020), Beijing Municipal Natural Science Foundation (Grant No.8214051).

REFERENCES

Abdullah J, Zaini SS, Aziz MSA, Majid TA, Yahya WM (2018) CFD Prediction on the pressure distribution and streamlines around an isolated single-storey house considering the effect of topographic characteristics. In: International Conference on Civil and Environmental Engineering for Sustainability. Malaysia, IOP Conference Series: Earth and Environmental Science, Proceedings...

AIJ-RLBC (2015) AIJ Recommendations for Loads on Buildings. Tokyo, Architectural Institute of Japan.

Bautista VL, Perea CAV, Osornio RC, García MC, Cantes GDJL (2016) Analysis coefficients wind force and flow behavior on a greenhouse model. Revista Mexicana de Ciencias Agrícolas 7(4): 821-832.

Blocken B, Hout A, Dekker J, Weiler O (2015) CFD simulation of wind flow over natural complex terrain: Case study with validation by field measurements for Ria de Ferrol, Galicia, Spain. Journal of Wind Engineering and Industrial Aerodynamics 147: 43-57.

Charisi S, Thiis TK, Aurlien T (2019) Full-scale measurements of wind-pressure coefficients in twin medium-rise buildings. Buildings 9(3): 63.

Chen P (2007) Numerical Study of Terrain Influence on the Airflow Over Hilly Land. Master Thesis, Zhejiang University, College of Architectural Engineering.

Feng HY, Su XB, Ma BL, Wang X (2016) Application of polyhedron grid in static aero-elastic computation. Flight Dynamics 4: 24-28.

GB 50009 (2012) Load code for the design of building structures. Beijing, China Architecture & Building Press.

Kim RW, Lee IB, Kwon KS (2017a) Evaluation of wind pressure acting on multi-span greenhouses using CFD technique, Part 1: Development of the CFD model. Biosystems Engineering 164: 235-256.

Kim RW, Hong SW, Lee IB, Kwon KS (2017b) Evaluation of wind pressure acting on multi-span greenhouses using CFD technique, Part 2: Application of the CFD model. Biosystems Engineering 164: 257-280.

Kwon K, Kim D, Kim R, Taehwan, Ha (2016) Evaluation of wind pressure coefficients of single-span greenhouses built on reclaimed coastal land using a large-sized wind tunnel. Biosystems Engineering 141: 58-81.

Lee I, Sase S, Okushima L, Ikeguchi A, Choi K (2003) A wind tunnel study of natural ventilation for multi-span greenhouse scale models using two-dimensional particle image velocimetry (PIV). Transactions of the ASAE 46(3): 763-772.

Moriyama H, Sase S, Uematsu Y, Ishii M, Okushima L (2015) Influence of ridge height of pipe-framed greenhouses on wind pressure coefficients. American Society of Agricultural and Biological Engineers 58(3): 763-769.

Paepe DM, Pieters JG, Cornelis WM, Gabriels C, Merci B (2013) Airflow measurements in and around scale-model cattle barns in a wind tunnel: Effect of wind incidence angle. Biosystems Engineering 115(2): 211-219.

Richards PJ, Hoxey RP (2012) Pressures on a cubic building—Part 1: Full-scale results. Journal of Wind Engineering and Industrial Aerodynamics 102: 72-86.

Shen GH, Yao D, Yu SC, Lou WJ, Xing YL (2016) Wind tunnel test of wind field characteristics on isolated hill and two adjacent hills. Journal of Zhejiang University (Engineering Science) 50(5): 805-812.

Sun Y (2011) Guide for wind tunnel testing of buildings. Beijing, China Architecture & Building Press.

Vieira Neto JG, Soriano J (2020) Computational modelling applied to predict the pressure coefficients in deformed single arch- shape greenhouses. Biosystems Engineering 200: 231-245.

Xiao YQ, Li C, Ou JP, Song LL, Li QS (2009) CFD approach to evaluation of wind energy in complex terrain. Journal of South China University of Technology (Natural Science Edition) 37(09): 30-35.

Yao D (2014) Research on characteristics of wind field on hilly terrain and its wind load effect on hilly terrain and its wind load effect. Master Thesis, Zhejiang University, College of Architectural Engineering.

Yao JF, Shen GH, Yao D, Xing YL, Lou WJ (2016) CFD-Based numerical simulation of wind field characteristics on valley and col terrain. Journal of Harbin Institute of Technology 48(12): 165-171.

Zhu ZW, Zhang SL, Liu ZQ, Chen ZQ (2011) CFD simulation of wind field at bridge site on gorge terrain. Journal of Hunan University (Natural Sciences) 38(10): 13-17.